Actinide cross sections from the reaction of ^{13}C with $^{254}Es^{g}$

K. J. Moody, R. W. Lougheed, R. J. Dougan, E. K. Hulet, J. F. Wild, K. Summerer,*
R. L. Hahn,† J. van Aarle,‡ and G. R. Bethune§
University of California, Lawrence Livermore National Laboratory, Livermore, California 94551
(Received 28 August 1989)

We have measured cross sections for the formation of actinide transfer products in the reaction of 72-MeV ^{13}C projectiles with $^{254}Es^{g}$ targets. The pattern of nuclide yields is similar to those observed in the reactions of heavier ions with $^{254}Es^{g}$. We have constructed the primary element yields from these results and show that the total cross section for transfer reactions is 58 mb. The total reaction cross section is about 300 mb. Lawrencium isotopes are formed with larger cross sections than are consistent with the trends of the transfer-product distributions; we explain this in terms of massive transfer, and model the lawrencium yields with an evaporation code.

I. INTRODUCTION

During the past several years, we have utilized targets of $^{254}Es^{g}$ to produce new nuclei and to explore a region of the chart of the nuclides that is inaccessible with any other target/projectile combination.[1-3] The $^{254}Es^{g}$ target material is the heaviest nuclide obtainable in quantities sufficient to be useful in heavy-ion reactions, where beam intensities are limited. Transfer reactions, in which there is an exchange of nucleons between the heavy-ion projectile and the target nucleus, have a special advantage in producing these very heavy isotopes: a larger fraction of the products, because of lower excitation energies, survive fission deexcitation than do the products of heavy-ion fusion reactions.

Transfer reactions with various actinide targets have been studied with projectiles ranging from ^{16}O to ^{238}U.[1,4-6] Transfer reactions with the heaviest projectiles (at energies near the interaction barrier) produce broad distributions of nuclides with atomic numbers both above and below that of the target. As the mass of the projectile decreases, the cross-section distributions become narrower, and the production of above-target nuclides dominates over below-target production, because of the driving force of the Coulomb potential toward charge asymmetry.[5]

In this paper, we report actinide cross sections from the reaction of ^{13}C ions with $^{254}Es^{g}$. This is the first comprehensive measurement of actinide transfer products with a projectile as light as ^{13}C. We have reconstructed the primary products of the reaction, based upon the observed products of their deexcitation, and have used this information to determine the total reaction cross section. We have interpreted the cross sections for the production of lawrencium isotopes, not only in terms of a transfer mechanism, but also from the standpoint of incomplete fusion or massive transfer.

II. EXPERIMENTAL

Irradiations were performed at the 88-in. Cyclotron at the Lawrence Berkeley Laboratory with beams of 84.4-MeV $^{13}C^{3+}$ ions. The beam was collimated to the 3 mm diameter of the $^{254}Es^{g}$ target and passed through a 4.5-mg/cm^2 molybdenum beam window, a volume of nitrogen cooling gas, and the target substrate before encountering the target material; the midtarget beam energy was degraded to 72 MeV.[7] The deposited electrical charge from the window outward to the beam dump was integrated and recorded periodically during irradiations to permit the reconstruction of the beam-intensity profiles.

The targets were prepared by electrodepositing $^{254}Es^{g}$ from isopropanol solutions of the chloride onto 4.5-mg/cm^2 molybdenum substrates. The deposits were overplated with 20 μg/cm^2 of palladium to reduce sputtering and thermal-evaporation losses. The target used in one set of bombardments was 57.8 μg/cm^2 of recently-prepared $^{254}Es^{g}$, which contained about 2.5 μg/cm^2 of ingrown ^{250}Cf. The target used in the second set of bombardments had decayed for several months prior to the experiments; at the time of the irradiations, it consisted of 40.4-μg/cm^2 $^{254}Es^{g}$ and 23.4-μg/cm^2 $^{249,250}Cf$. Only negligible amounts (by mass) of other isotopes of einsteinium were present in either target.

Prior to collection, reaction products recoiling out of the target passed through the palladium overcoating and a free-standing 50-μg/cm^2 aluminum cover foil. These cover foils served to further decrease the contamination of the recoil-collecting media with thermally-evaporated target material. The recoils were stopped in either 4.5-mg/cm^2 molybdenum catcher foils, or in a volume of 1.4-atm helium gas containing a KCl aerosol. The catcher foils subtended laboratory angles out to about 55° from the beam axis. This is very nearly the same angle beyond which elastically-recoiling target atoms were stopped before leaving the cover foil; therefore, the range of angles from which recoils were collected was nearly the same no matter whether the solid or the gaseous stopping medium was employed.

Catcher foils were removed from the vicinity of the target following irradiations between 10 min and 8 h in length. Some of these foils were inserted into counters immediately without further treatment. Others were chemically processed, and the isolated actinide fractions were then counted. In this latter procedure, the catcher

foils were dissolved in aqua regia, and the resultant solution was passed through an anion-exchange column that removed the bulk of the molybdenum. The column eluant was evaporated to dryness and loaded on an alpha-hydroxyisobutyrate cation-exchange column. Fractions containing lawrencium, mendelevium, fermium, and einsteinium were collected from the column. It was necessary to repeat the procedure on the lawrencium fraction to ensure that it was free of other actinides so that very-low-level spontaneous fission activities[8] could be observed. Fractions were evaporated on platinum disks that were brought to red heat prior to counting. This procedure took about an hour to perform.

In experiments where the recoiling reaction products were stopped in helium gas, the contents of the recoil chamber were continuously pumped through a capillary while fresh KCl-laden helium was supplied. Actinide reaction products attached themselves to the aerosol particles, which were swept through the 1-mm-diameter, 3-m-long capillary and then deposited on 30-$\mu g/cm^2$ polypropylene foils in the Multiple Alpha Detector (MAD) system.[9] The overall efficiency for the collection/deposition process was 64%, determined by comparing the ^{256}Fm spontaneous-fission activity from the catcher foils (assumed to be 100% efficient) with the same activity deposited on a MAD foil that was retrieved and counted off line. In the MAD system, activity was deposited sequentially on a series of thin foils that were stepped between opposing pairs of surface-barrier detectors. The energy, detector number, and running time of each alpha-particle event were stored on magnetic tape. These data were later converted into spectra as a function of time after deposition on each foil.

After the MAD experiments, some of the plastic foils were dismounted from the wheel and counted off line. Most of the foils were collected and washed, and the resultant solution was reduced in volume and processed according to the chemical procedure outlined earlier. The mendelevium, fermium, and einsteinium fractions were evaporated on platinum disks that were then brought to red heat.

We counted all off-line samples for alpha particles and spontaneous-fission events with surface-barrier detectors. The pulse-height spectra were recorded periodically for as long as 10 months after the irradiations.

III. DATA TREATMENT AND RESULTS

Intensity peaks in the alpha spectra were integrated and used to construct decay curves. Initial activities and beam-intensity histories were used to calculate production cross sections. These cross sections are listed in Table I and plotted in Fig. 1 as a function of mass number. Corrections have been made to the ^{256}Fm and ^{257}Fm cross sections for ingrowth from $^{256}Es^{m+g}$, ^{256}Md, and ^{257}Md during the irradiations and prior to any chemical separations. It has been assumed that reactions with the ^{250}Cf present in the target in the first set of bombardments did not contribute to the observed activities, since it constituted only 4% of the target material and is further removed in neutron and proton numbers from the observed reaction products than is $^{254}Es^{g}$. In the second set of bombardments, where there was substantial californium in the target, there was the possibility that $^{13}C+Cf$ reactions might contribute significantly to the yields of the more neutron-deficient transfer products we observed; therefore, these cross sections were excluded from the final set. Cross sections determined from chemically-separated samples were normalized to the results obtained from counting unseparated catcher foils. In cases where a given cross section was determined in more than one experiment, a weighted average of the values is given.

We were unable to determine cross sections for the reactions of $^{13}C+^{254}Es^{g}$ leading to below-target nuclides (californium and berkelium isotopes), because of the direct production of these nuclides from ^{250}Cf in the target and their formation from the decay of the einsteinium and fermium reaction products. We expect these cross sections to be small, as inferred from below-target nuclide yields from other reactions with actinide targets.[5,10]

TABLE I. Cross sections for the production of heavy nuclides in the reaction of 72-MeV ^{13}C ions with $^{254}Es^{g}$. The cross sections have been corrected for ingrowth from parent activities and for contributions from reactions with actinide impurities in the target.

Nuclide	Cross section (cm^2)
^{252}Es	$(3.64\pm0.51)\times10^{-27}$
^{253}Es	$(1.32\pm0.17)\times10^{-26}$
$^{254}Es^{g}$	$(4.63\pm0.54)\times10^{-25}$
$^{254}Es^{m}$	$(8.42\pm1.24)\times10^{-27}$
^{255}Es	$(1.79\pm0.19)\times10^{-26}$
$^{256}Es^{g}$	$(7.3\pm2.6)\times10^{-30}$
$^{256}Es^{m}$	$(1.54\pm0.42)\times10^{-29}$
^{253}Fm	$(3.0\pm0.5)\times10^{-28}$
^{254}Fm	$(1.76\pm0.24)\times10^{-27}$
^{255}Fm	$(2.47\pm0.34)\times10^{-27}$
^{256}Fm	$(7.77\pm0.82)\times10^{-28}$
^{257}Fm	$(2.01\pm0.14)\times10^{-28}$
^{255}Md	$(7.6\pm1.4)\times10^{-30}$
^{256}Md	$(4.13\pm0.42)\times10^{-29}$
^{257}Md	$(6.79\pm0.68)\times10^{-29}$
$^{258}Md^{g}$	$(2.11\pm0.21)\times10^{-29}$
^{260}Md	$\leq2.4\times10^{-32}$
^{256}No	$\leq8\times10^{-33}$
^{257}No	$(1.2\pm0.4)\times10^{-32}$
^{259}No	$\leq7\times10^{-31}$
^{259}Lr	$\leq6.4\times10^{-33}$
^{260}Lr	$(7.6\pm2.4)\times10^{-32}$
^{261}Lr	approx. 3×10^{-32}
^{262}Lr	approx. 1.5×10^{-33}
$^{261}104$	$\leq9\times10^{-33}$
$^{262}105$	$\leq8\times10^{-33}$

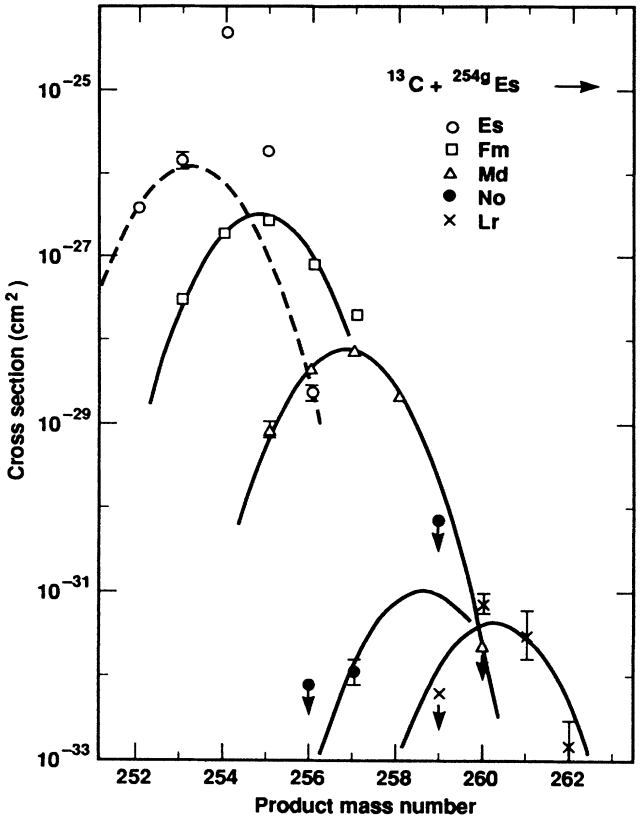

FIG. 1. Cross sections for the production of actinide nuclides from the reaction of 72-MeV ^{13}C with $^{254}Es^g$. Gaussian curves with 1.89 u full width at half maximum (FWHM) are drawn through the data for each element. The position of the peak of the Gaussian curve shown for nobelium isotopes is calculated as described in the text.

IV. DISCUSSION

A. Actinide cross sections

The cross sections in Fig. 1 are shown overlaid with Gaussian distributions with width parameters $\sigma^2=0.65$ u^2 (full width at half maximum, FWHM=1.89 u). This is significantly narrower than the $\sigma^2=0.914$ u^2 curves found to fit cross-section distributions from 127-MeV ^{22}Ne reactions with $^{254}Es^g$.[1] This is reasonable, not only because of the lower projectile mass, but also because of the relative reaction energies and their proximities to the interaction barriers; 72-MeV ^{13}C ions are only 1% more energetic than the spherical Coulomb barrier, while 127-MeV ^{22}Ne ions are 8% more energetic. Our transfer-product measurements were performed in conjunction with a search for the complete-fusion products $^{263}105$ and $^{264}105$. We chose a low beam energy to maximize the yields of those nuclides. The results of that search will be presented in a subsequent paper.

Cross sections for $^{254}Es^{m+g}$ and ^{255}Es were excluded from the Gaussian fit to the einsteinium reaction products since they are produced by more peripheral reaction mechanisms (e.g., elastic scattering, single-nucleon transfer, or quasielastic transfer[11,12]). A distribution was assigned to nobelium by requiring the peak cross section to fall at mass number 258.6, a value derived by fitting with a straight line the most-probable masses of the other Gaussian distributions as a function of atomic number, as shown in Fig. 2. We discuss the validity of this assumption below, in Sec. IV D.

The heights of the isotopic distributions decrease in a uniform way, except for the large gap between the $\Delta Z=2$ (mendelevium) and $\Delta Z=3$ (nobelium) distributions. This "odd-even" effect has also been observed in the reactions of ^{18}O and ^{22}Ne ions with $^{254}Es^g$ (Ref. 1) and other actinide targets.[4,10] The gap results from an increase in the intrinsic excitation energy of the primary actinide products of the reaction with increasing transfer of charge from the projectile to the target (see below).

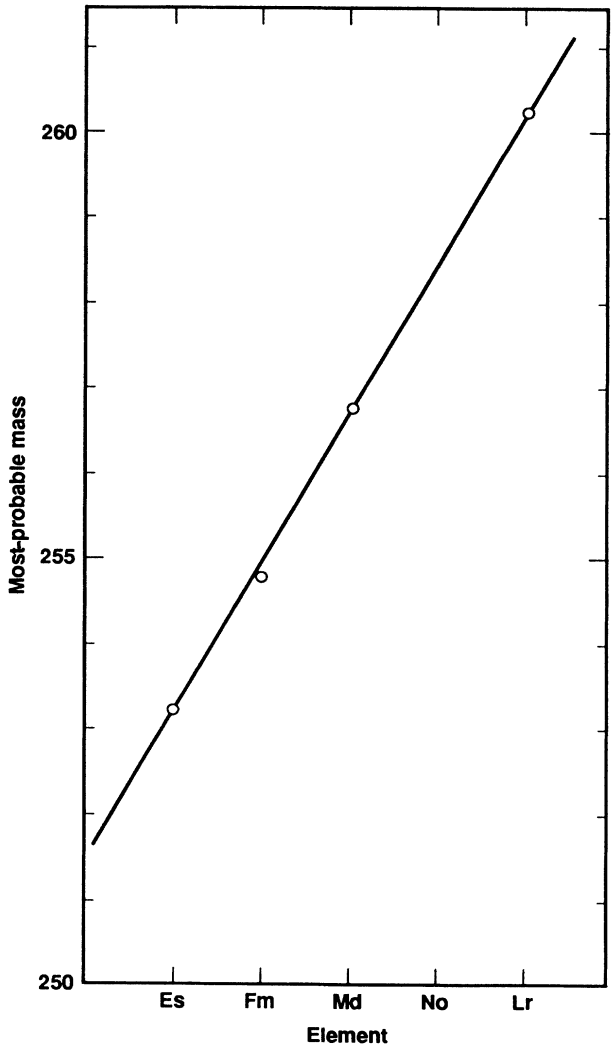

FIG. 2. Most-probable nuclide masses obtained from the Gaussian distributions in Fig. 1 as a function of atomic number. We expect the most-probable mass of the nobelium distribution to be 258.6 u.

B. Primary product distributions

In Fig. 3, we plot the energy excess for the formation of various primary actinide products of the reaction of 72-MeV ^{13}C ions with $^{254}Es^{g}$. In calculating these numbers, we made two assumptions: no particle evaporation prior to separation of the reacting system into projectile- and target-like primary products in the exit channel, and spherical Coulomb barriers in the exit channel. The energy excess, E_{ex}, is given by

$$E_{ex}=Q+E_{c.m.}-E_{Coul,exit}\ , \tag{1}$$

where $E_{Coul,exit}$ is the Coulomb energy at separation in the exit channel, and $E_{c.m.}$ is the center-of-mass reaction energy. The excess energy over the Coulomb potential is available as excitation energy of the primary actinide product. We used the parametrization of Lefort[13] to determine the interaction radii. Mass excess values from Refs. 14 and 15 were used in the Q-value calculations.

If the assumption of spherical barriers was exact, products for which there is a negative energy excess would be inaccessible to the reaction as final products. Since the possible excitation energies are fairly small, we can assume that the deformations of the primary actinide fragments are about the same as their ground-state deformations. The droplet model[16] gives $\alpha=0.18$–0.19 for these nuclei, corresponding to a prolate radius[17] of 1.20 times the spherical radius and a decrease in the exit-channel Coulomb barrier of about 7 MeV (for einsteinium products) to about 3 MeV (for lawrencium products); this energy is available as excitation energy. We have not included this extra energy from deformation in the data plotted in Fig. 3.

For each element, two mass numbers are indicated with arrows in Fig. 3. The arrows on the left indicate the positions of the peaks of the isotopic distributions of the final reaction products (from Figs. 1 and 2). The arrows on the right indicate the mass at which the energy excess is at a maximum for that element, taken from parabolic fits to the data in Fig. 3. This corresponds to the minimum potential energy (MPE) for forming a primary reaction product with that atomic number.[18–20]

In Fig. 4, we plot the most-probable masses of the observed reaction products against atomic number (element) along with the most-probable masses of primary reaction products calculated under three different hypotheses: using MPE (explained previously), which is derived from the data in Fig. 3; using uniform charge density (UCD), in which nuclear charge is distributed between the target-like and projectile-like reaction components according to their masses just prior to separation of the reaction intermediate; and using target-plus-projectile

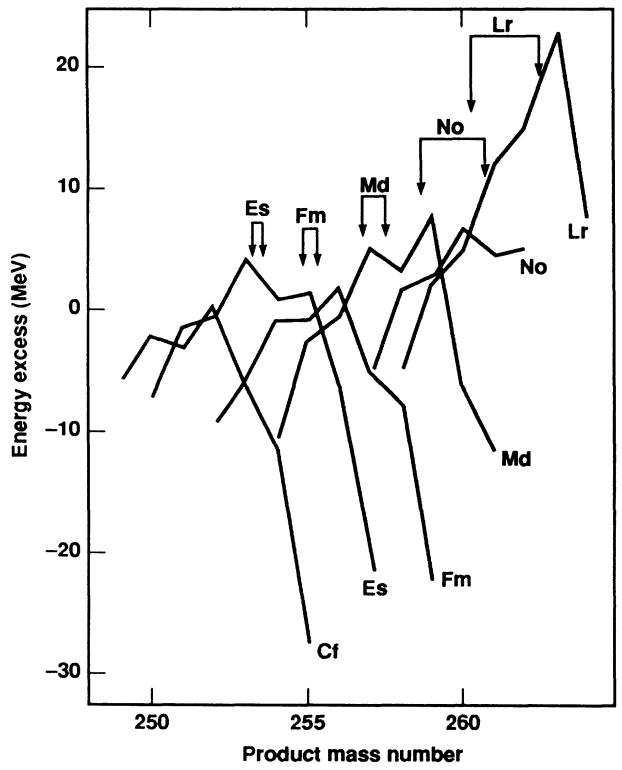

FIG. 3. Energy excess for binary reactions resulting in the primary products indicated. The calculation assumes spherical Coulomb barriers in the exit channels. Arrows indicate the most-probable masses of observed reaction products (left) and the mass of greatest energy excess for that atomic number (right). These latter values were obtained from a parabolic fit to the data in the figure.

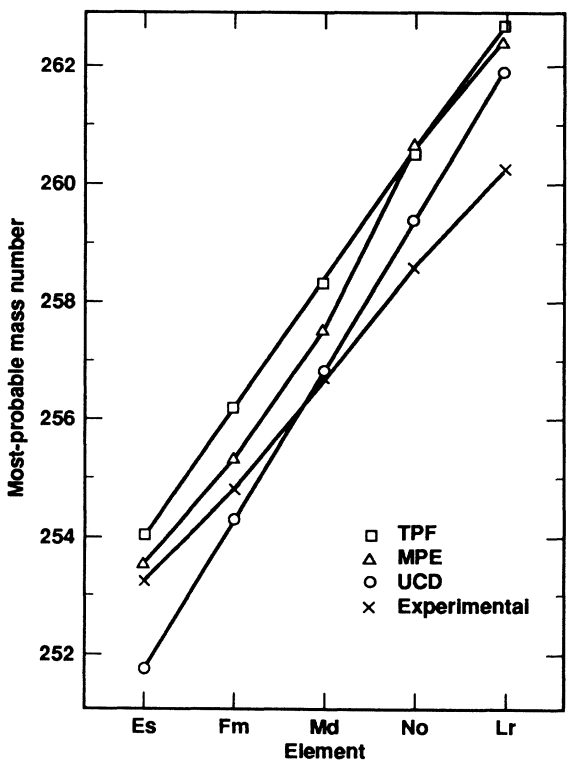

FIG. 4. Most-probable masses as a function of atomic number. Experimental data is displayed along with the most-probable masses of the primary-reaction-product distributions calculated by three different methods that are described in the text.

fragment (TPF), in which transfer of a given number of protons to the target carries with it a most-probable number of neutrons determined by the charge-to-mass ratio of the projectile. As the size of the transfer increases toward formation of a compound nucleus, the results of the three calculations converge, as shown in Fig. 4.

Fission widths relative to neutron-emission widths[21,22] are only slowly changing with mass at constant Z for the observed products (all are beyond the 152 neutron shell). Therefore, the differences between the most-probable masses of the observed distributions and those of the primary distributions give a rough measure of the number of neutrons emitted in the deexcitation of the primary fragments.

With a reacting system as asymmetric as this one, we expect that the net exchange of charge goes strongly in the projectile-to-target direction.[5] With this one-directional flow, and with the limited duration of the reaction intermediate,[18] we would expect both MPE and TPF to be better models than UCD for reproducing the most-probable mass numbers of the primary actinide products. This is true, clearly, for the predicted peaks of the einsteinium, fermium, and mendelevium primary mass distributions, for which UCD predicts mass numbers lower than or equal to those observed for the final reaction products. We prefer the use of MPE over TPF because, even in a one-directional transfer, contact of nuclear matter provides for charge exchange.[18] Thus, in the calculations that follow, we use the MPE assumption to determine the most-probable masses of the primary-product distributions.

The neutron separation energies for our product nuclei lie around 5–7 MeV, depending upon whether the neutron number is odd or even.[14] We see very little shift ($\sim$0.3 u) between the expected peak of the primary distribution of einsteinium isotopes and the observed isotope distribution, though as much as 12 MeV (Fig. 3 plus energy from Coulomb barrier deformation) is available as excitation energy. Very little of the energy excess is converted from kinetic energy in the entrance channel into excitation energy in the exit channel. For the production of mendelevium isotopes, where a similar amount of energy is available, Figs. 3 and 4 indicate that the primary-to-observed distribution shift is about 0.75 u, corresponding to a greater damping of kinetic energy into excitation energy. The shift indicated for nobelium isotopes is approximately 2 u; hence, a large jump in excitation energy, a large increase in the probability of fission in the deexcitation process, and the observed drop in yield from mendelevium to nobelium.

C. Transfer reaction and total reaction cross sections

From the estimates of the average numbers of neutrons emitted in the formation of the final reaction products, we can use the relative fission and neutron-emission widths of Sikkeland *et al.*[21,23] to determine the total cross section for the primary-product distribution of each element:

$$\sigma_{\text{primary}} = \sigma_{\text{observed}}[(\Gamma_f + \Gamma_n)/\Gamma_n]^x , \quad (2)$$

where Γ_f and Γ_n are the fission and neutron-emission widths, respectively, for the most-probable primary product at a particular Z, and x is the average number of emitted neutrons. In Table II, the Gaussian distributions shown in Fig. 1 are integrated to give the observed yield for each element. The average numbers of emitted neutrons are defined by the differences between the peaks of the observed isotope distributions (Fig. 2) and the most-probable masses calculated under the MPE assumption (Fig. 3). Since a certain number of neutrons were emitted to give the observed distributions, the relative decay widths yield the number of fissioned nuclei for each final product atom. This gives the primary-product yields listed in Table II. The primary transfer cross section is about 58 mb; provided this is correct, we can estimate the total reaction cross section by calculating its other components.

There are some einsteinium products formed from more peripheral reactions that were not included in the Gaussian fit to the transfer-product cross sections. These nuclides arise from elastic and inelastic scattering and from neutron pickup from the odd-n ^{13}C projectile. We assume that the target thickness and the palladium overcoating preclude significant contributions from secondary reactions. We also assume that the excitation energies of these products are so low that fission does not play a role in their deexcitation. The cross section for producing ^{254}Es^{g}, which we report on the basis of five different experiments that gave the same result, has contributions from both nuclear scattering and from elastic (Rutherford) scattering at larger impact parameters. We believe there is no contribution from simple contamination or from thermal transfer of activity through the target overcoating and the aluminum cover foil, based on the equivalence of the five separate determinations.

Those portions of the cross sections for ^{255}Es and ^{254}Es^{m} in excess of the transfer reaction Gaussian sum to

TABLE II. Element yields for actinide transfer products of the reaction of 72-MeV ^{13}C ions with ^{254}Es^{g}. Observed yields are obtained by integrating the Gaussian distributions in Fig. 1. Using the most-probable masses (MPE) from Fig. 4, we estimate the cross section for the primary production of each element in the reaction prior to deexcitation by fission and neutron emission, as described in the text.

Element	Observed yield (cm^2)	Average emitted neutrons	Primary yield (cm^2)
Lr	1×10^{-31}	2.15	4×10^{-30}
No	2×10^{-31}	2.0	4×10^{-30}
Md	1.4×10^{-28}	0.75	8.6×10^{-28}
Fm	6.7×10^{-27}	0.5	2.1×10^{-26}
Es	2.38×10^{-26}	0.3	3.6×10^{-26}
Cf[a]	$\sim7\times10^{-29}$		
Bk[a]	$\sim1\times10^{-29}$		
Total	3.07×10^{-26}		5.8×10^{-26}

[a]Estimated (from Refs. 1, 5, and 10).

TABLE III. Itemization of the total reaction cross section for the interaction of 72-MeV ^{13}C ions with $^{254}Es^{g}$.

Reaction type	Cross section (mb)	
Primary transfer		58
Fusion (estimated)		5
Excess ^{255}Es and $^{254}Es^{m}$		22
Excess $^{254}Es^{g}$	460	
Rutherford	−240	
Net reaction $^{254}Es^{g}$		220
Reaction cross section		305 mb

22 mb. The excess $^{254}Es^{g}$ cross section is 460 mb. We calculate that the Rutherford scattering cross section,[24] integrated between target-recoil laboratory angles of 0° and 55° (see above) is 240 mb. This leaves a net $^{254}Es^{g}$ nuclear reaction cross section of about 220 mb.

We calculate[25] that the classical cross section for the fusion of 72-MeV ^{13}C ions with $^{254}Es^{g}$ is about 5 mb. In Table III we sum up all the reaction components: the total reaction cross section is about 300 mb. We assume that direct fission processes like Coulomb fission do not contribute significantly to the cross section.[26] The reaction cross section we obtain is considerably greater than the 21 mb we calculate from the Fresnel model[25,27] assuming spherical nuclei. With the ingoing-wave strong-absorption model,[28] which takes into account the deformations of the interacting nuclei, we calculate a total reaction cross section of about 10 mb. Two factors that might account for the discrepancy between the calculated and derived total reaction cross sections are: (a) that quantum-mechanical barrier penetration significantly enhances the cross section relative to the results of classical calculations for reaction energies near the interaction barrier;[29] and (b) that a small error in the determination of the projectile energy can have a large effect on the near-barrier cross sections.

D. Formation of lawrencium isotopes.

Primary element yields from Table II are plotted against atomic number (element) in Fig. 5. The yields fall off in a regular way with increasing transfers of charge to the target, until lawrencium ($\Delta Z=4$) is reached. Clearly, there is a difference in the production mechanism through which most of the lawrencium cross section arises. The lawrencium isotopes can be described as the products of (heavy-ion, αxn) reactions.

The excitations functions for the products of (heavy-ion, αxn) reactions with actinide targets are broader than those observed in the same reaction system for (heavy-ion, xn) products,[30] though not as broad as the excitation functions for lighter transfer products.[31] Peak cross sections for actinide (heavy-ion, αxn) products are substantially larger than those for (heavy-ion, xn) products from the same reacting system and with the same number of emitted neutrons.[30,32] In 1958, on the basis of these observations, Sikkeland *et al.*[30] proposed a mechanism in

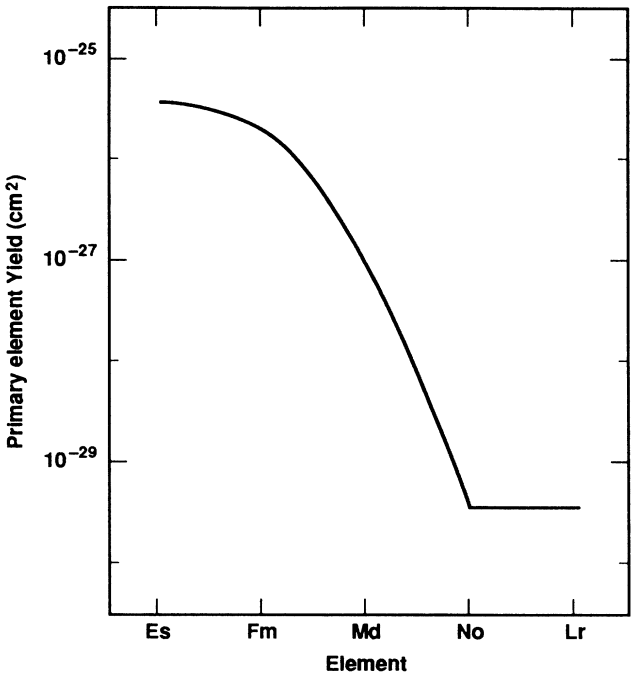

FIG. 5. Primary reaction cross sections for elements produced in the reaction of 72-MeV ^{13}C with $^{254}Es^{g}$, plotted against atomic number.

which the alpha particle was ejected prior to the fusion of the projectile residue with the target nucleus. This is consistent with the later observation in similar reactions of light fragments ($A \leq 4$) emitted in the forward direction with energies that are much higher than those expected from particle evaporation from hot nuclei.[33,34]

A mechanism called massive transfer[35] or incomplete fusion has been proposed for the formation of the products of (heavy-ion, αxn) reactions. Massive transfer occurs for collisions with a small range of impact parameters, with angular momenta near the critical angular momentum for fusion.[35] The primary products of the fusion of the projectile residue with the target nucleus have a range of excitation energies, since the alpha particles are emitted without well-defined momenta.[35,36] Massive transfer has been treated as the extreme limit of transfer or deep-inelastic reactions[37] since the angular momenta for the process are closely confined between those for fusion and the broad range of angular momenta arising in transfer reactions.[38] However, massive transfer occurs only in reactions with projectiles lighter than ^{40}Ar (Ref. 35); this implies that the nuclear structure of the projectile plays a part in the initial ejection of the alpha particle. Though not an alpha-cluster nucleus, ^{13}C is stable to emission of an alpha particle by only 10.7 MeV,[39] which is considerably less than the potential energy available in the entrance channel of our reaction.

We do not favor the assumption of an entirely different mechanism for (heavy-ion, αxn) reactions. It seems somewhat arbitrary to distinguish reactions occurring within a narrow window of angular momentum as being

discrete from reactions occurring at both larger and smaller impact parameters. We feel that massive transfer is part of the continuum of reaction mechanism that spans the domain from few-nucleon transfer to the formation of a complete-fusion nucleus. The (heavy-ion, αxn) reaction is an extreme case of transfer reaction, whose probability is enhanced by the nuclear structure of the projectile. This is supported by excitation functions[30,31] and by the systematic trend of the most-probable masses for a given Z, plotted in Fig. 2. This justifies the use of Fig. 2 to define the peak position of the nobelium distribution (Sec. IV A).

The simplicity of the reacting system in the exit channels leading to lawrencium isotopes lets us model their production with the evaporation code SPIT (Ref. 40). SPIT assumes formation of a complete-fusion nucleus that deexcites by neutron emission or fission. The relative widths for the two deexcitation processes are taken from the empirical angular momentum and excitation energy independent Sikkeland systematics.[21,23] The calculation allows no angular momentum to be carried off by evaporated neutrons, and only neutrons are emitted in competition with fission until the entry line to the Yrast band is reached, where gamma-ray emission predominates.

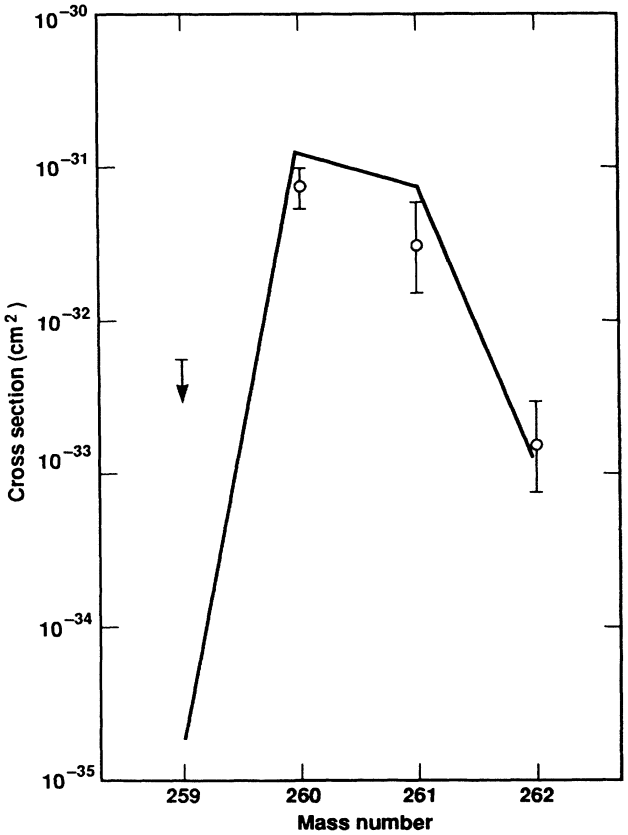

FIG. 6. Experimental cross sections for the production of lawrencium isotopes in the reaction of 72-MeV ^{13}C ions with ^{254}Es^g, compared with the results of a SPIT calculation (solid line) that have been scaled by 0.021.

This simple code has been surprisingly successful in calculating (heavy-ion, xn) actinide cross sections.[40]

For (heavy-ion, αxn) cross sections, SPIT assumes that the primary actinide product is formed after emission of an alpha particle from the projectile, by the fusion of the projectile residue with the target. The excitation energy of this product is determined by the kinematics of the binary reaction: the alpha particle is assumed to be emitted in the beam direction with the velocity of the projectile. The angular momentum distribution of the heavy primary product is taken to be that of the complete-fusion nucleus. The results of SPIT calculations of cross sections for (heavy-ion, αxn) products tend to be larger than those determined experimentally. The code assumes that the entire complete-fusion cross section results in the (heavy-ion, αxn) precursor, rather than taking as input an appropriately small fraction of the transfer-reaction cross section. Also, the assumed kinetic energy of the alpha-particle spectator yields the minimum excitation energy in the heavy primary product rather than a more realistic distribution of higher excitation energies.

Primary products on the lower edge of the excitation energy distribution contribute disproportionately to the products which survive fission deexcitation; therefore, we would expect SPIT to adequately reproduce the shape of the cross section distribution for lawrencium isotopes, though not its magnitude. In Fig. 6, we plot our experimental lawrencium cross sections with those calculated with SPIT, scaled by 0.021, shown as a solid line. The agreement between the shapes of the measured and calculated distributions is surprisingly good.

V. CONCLUSIONS

We have measured the cross sections for the production of actinide nuclides in the reaction of 72-MeV ^{13}C ions with ^{254}Es^g. The FWHM of the isotopic distributions is 1.89 u, considerably narrower than similar distributions arising from the interactions of higher-energy heavier ions with ^{254}Es^g. By assuming the minimization of potential energy, we have calculated the most-probable mass for each element; we attribute deviations of the peaks of the experimental distributions from these masses to the evaporation of neutrons. This treatment gives a qualitative explanation of the magnitude of the gap between the isotopic distributions of mendelevium and nobelium. In these transfer reactions, considerably more energy is available than is damped into excitation energy of the primary transfer products.

We calculate the primary transfer-product yield to be 58 mb. Using a calculated fusion cross section and the cross sections of products from peripheral reactions, we estimate a total reaction cross section of 300 mb. This is considerably greater than the cross section calculated for this reaction using classical physics models.

An apparent enhancement of lawrencium yields relative to those expected from the trend of the other actinide cross sections indicates a change in mechanism leading to the formation of these nuclides. We attribute this to nuclear structure in the projectile, responsible for the release of an alpha particle prior to fusion of the projec-

tile residue with the target. We were able to reproduce the lawrencium isotopic distribution with an evaporation code, assuming the initial loss of an alpha particle, emitted in the forward direction with the beam velocity.

ACKNOWLEDGMENTS

We would like to thank the staff and crew of the 88-in cyclotron for their interest and assistance. We would also like to thank Edward Watkins for his electronics expertise during our Multiple Alpha Detector (MAD) wheel experiments. We are indebted for the use of the target material to the Office of Basic Energy Sciences, U.S. Department of Energy, through the transplutonium production facilities of the Oak Ridge National Laboratory. This research was performed under the auspices of the U.S. Department of Energy by the Lawrence Livermore National Laboratory under Contract No. W-7405-Eng-48.

---

*Also at Gesellschaft für Schwerionenforschung, Darmstadt, Federal Republic of Germany.

†Also at Chemistry Department, Brookhaven National Laboratory, Upton, NY 11973.

‡Present address: Universität Marburg, Federal Republic of Germany.

§Deceased.

[1]M. Schädel, W. Brüchle, M. Brügger, H. Gäggeler, K. J. Moody, D. Schardt, K. Sümmerer, E. K. Hulet, A. D. Dougan, R. J. Dougan, J. H. Landrum, R. W. Lougheed, J. F. Wild, and G. D. O'Kelley, Phys. Rev. C **33**, 1547 (1986).

[2]R. W. Lougheed, E. K. Hulet, R. J. Dougan, J. F. Wild, R. J. Dupzyk, C. M. Henderson, K. J. Moody, R. L. Hahn, K. Sümmerer, and G. Bethune, J. Less-Common Met. **122**, 461 (1986).

[3]E. K. Hulet, R. W. Lougheed, J. F. Wild, R. J. Dougan, K. J. Moody, R. L. Hahn, C. M. Henderson, R. J. Dupzyk, and G. R. Bethune, Phys. Rev. C **34**, 1394 (1986).

[4]D. Lee, H. R. von Gunten, B. Jacak, M. Nurmia, Y.-F. Liu, C. Luo, G. T. Seaborg, and D. C. Hoffman, Phys. Rev. C **25**, 286 (1982).

[5]K. J. Moody, D. Lee, R. B. Welch, K. E. Gregorich, G. T. Seaborg, R. W. Lougheed, and E. K. Hulet, Phys. Rev. C **33**, 1315 (1986).

[6]M. Schädel, W. Brüchle, H. Gäggeler, J. V. Kratz, K. Sümmerer, G. Wirth, G. Herrmann, R. Stakemann, G. Tittel, N. Trautmann, J. M. Nitschke, E. K. Hulet, R. W. Lougheed, R. L. Hahn, and R. Ferguson, Phys. Rev. Lett. **48**, 852 (1982).

[7]F. Hubert, A. Fleury, R. Bimbot, and D. Gàrdes, Ann. Phys. (Paris), Suppl. **5**, 1 (1980).

[8]R. W. Lougheed, K. J. Moody, R. J. Dougan, J. F. Wild, E. K. Hulet, R. J. Dupzyk, C. M. Henderson, C. M. Gannett, R. A. Henderson, D. C. Hoffman, D. M. Lee, K. Sümmerer, and R. L. Hahn, Lawrence Livermore National Laboratory, Nuclear Chemistry Division FY87 Annual Report No. UCAR 10062/87, 1987, p. 4–2.

[9]R. J. Dougan, R. W. Lougheed, E. K. Hulet, and G. R. Bethune, Lawrence Livermore National Laboratory, Nuclear Chemistry Division FY84 Annual Report No. UCAR 10062-84/1, 1984, p. 2–15.

[10]D. Lee, K. J. Moody, M. J. Nurmia, G. T. Seaborg, H. R. von Gunten, and D. C. Hoffman, Phys. Rev. C **27**, 2656 (1983).

[11]V. V. Volkov, G. F. Gridnev, G. N. Zorin, and L. P. Chelnokov, Nucl. Phys. **A126**, 1 (1969).

[12]U. Reus, A. M. H. Wätzig, R. A. Esterlund, P. Patzelt, and I. S. Grant, Phys. Rev. Lett. **39**, 171 (1977).

[13]M. Lefort, Rep. Prog. Phys. **39**, 129 (1976).

[14]A. H. Wapstra and G. Audi, Nucl. Phys. **A432**, 1 (1985).

[15]S. Liran and N. Zeldes, At. Data Nucl. Data Tables **17**, 431 (1976).

[16]W. D. Myers, *Droplet Model of Atomic Nuclei* (IFI/Plenum, New York, 1977).

[17]A. Bohr and B. R. Mottelson, Dan. Mat.-Fys. Medd. **30**, 1 (1955).

[18]H. Freiesleben and J. V. Kratz, Phys. Rep. **106**, 1 (1984).

[19]H. Gäggeler, W. Brüchle, M. Brügger, M. Schädel, K. Sümmerer, G. Wirth, J. V. Kratz, M. Lerch, T. Blaich, G. Herrmann, N. Hildebrand, N. Trautmann, D. Lee, K. J. Moody, K. E. Gregorich, R. B. Welch, G. T. Seaborg, D. C. Hoffman, W. R. Daniels, M. M. Fowler, and H. R. von Gunten, Phys. Rev. C **33**, 1983 (1986).

[20]R. B. Welch, K. J. Moody, K. E. Gregorich, D. Lee, and G. T. Seaborg, Phys. Rev. C **35**, 204 (1987).

[21]T. Sikkeland, A. Ghiorso, and M. J. Nurmia, Phys. Rev. **172**, 1232 (1968).

[22]E. A. Cherepanov, A. S. Iljinov, and M. V. Mebel, J. Phys. G **9**, 931 (1983).

[23]T. Sikkeland, J. Maly, and D. F. Lebeck, Phys. Rev. **169**, 1000 (1968).

[24]P. Marmier and E. Sheldon, *Physics of Nuclei and Particles* (Academic, New York, 1969), Vol. 1, Chap. 3, and Appendix C.

[25]W. W. Wilcke, J. R. Birkelund, H. J. Wollersheim, A. D. Hoover, J. R. Huizenga, W. U. Schröder, and L. E. Tubbs, At. Data Nucl. Data Tables **25**, 389 (1980).

[26]H. Holm and W. Greiner, Nucl. Phys. **A195**, 333 (1972).

[27]W. E. Frahn, Nucl. Phys. **A302**, 267 (1978).

[28]C. Y. Wong, Phys. Rev. Lett. **31**, 766 (1973).

[29]R. Bass, *Nuclear Reactions with Heavy Ions* (Springer-Verlag, Berlin, 1980), Chap. 3.

[30]T. Sikkeland, S. G. Thompson, and A. Ghiorso, Phys. Rev. **112**, 543 (1958).

[31]P. Eskola, K. Eskola, M. Nurmia, and A. Ghiorso, Phys. Rev. C **2**, 1058 (1970).

[32]G. N. Flerov, Yu. Ts. Oganesian, Yu. V. Lobanov, Yu. A. Lasarev, S. P. Tretiakova, I. V. Kolesov, and V. M. Plotko, Nucl. Phys. **A160**, 181 (1971).

[33]H. C. Britt and A. R. Quinton, Phys. Rev. **124**, 877 (1961).

[34]T. Inamura, M. Ishihara, T. Fukuda, and T. Shimoda, Phys. Lett. **68B**, 51 (1977).

[35]D. R. Zolnowksi, H. Yamada, S. E. Cala, A. C. Kahler, and T. T. Sugihara, Phys. Rev. Lett. **41**, 92 (1978).

[36]T. Inamura, A. C. Kahler, D. R. Zolnowski, U. Garg, T. T. Sugihara, and M. Wakai, Phys. Rev. C **32**, 1539 (1985).

[37]M. Lefort, Rep. Prog. Phys. **39**, 9 (1976).

[38]W. U. Schröder and J. R. Huizenga, Annu. Rev. Nucl. Sci. **27**, 465 (1977).

[39]*Table of Isotopes*, edited by C. M. Lederer and V. S. Shirley, 7th ed. (Wiley, New York, 1978).

[40]G. R. Haynes, J. D. Leyba, and D. C. Hoffman, private communication.